Available online at www.sciencedirect.com
SCIENCE DIRECT®
Journal of Molecular Spectroscopy 227 (2004) 151–157
Journal of MOLECULAR SPECTROSCOPY
www.elsevier.com/locate/jms

High resolution Fourier transform spectrum of HDO in the 7500–8200 cm^{-1} region: revisited☆

O.V. Naumenko,[a] S. Voronina,[a] and S.-M. Hu[b,*]

[a] *Institute of Atmospheric Optics, SB, Russian Academy of Science, Tomsk, Russia*
[b] *Laboratory of Bond Selective Chemistry, University of Science and Technology of China, Hefei 230026, China*

Received 6 March 2004
Available online 3 July 2004

Abstract

The HDO absorption FT spectrum is recorded and analyzed in the 7500–8200 cm^{-1} spectral region. The high accuracy ab initio calculation of Schwenke and Partridge was successfully applied for spectrum assignment that resulted in derivation of 508 precise rovibrational energy levels for the (3 0 0), (0 3 1), (1 1 1), (0 6 0), (2 2 0), and (0 0 2) states, with 295 of them being reported for the first time. In particular, eight new energy levels, including the band center at 7914.3170 cm^{-1}, were derived for the highly excited bending (0 6 0) state from transitions borrowing their intensities through local high-order resonance coupling with the (3 0 0) and (0 3 1) states.

Keywords: Vibration–rotation spectra; HDO molecule; Water absorption

1. Introduction

Extensive calculations of the water vapor and its isotope species' line positions and intensities performed by Schwenke and Partridge (SP) [1,2] initiated numerous theoretical and experimental investigations of the water vapor absorption spectra in different spectral regions. The ab initio calculations by SP and more recently by Polyansky et al. [3,4] are very attractive for applications due to their high accuracy in terms of line position and intensity. At the same time the effective Hamiltonian (EH) approach traditionally used for the high resolution spectra modeling often meets with difficulties when applied to the highly excited interacting vibrational states of nonrigid molecules like water. The main problems in the EH method come from the divergence of the perturbation series in the presentation of the rotational Hamiltonian, as well as strong and numerous interpolyad resonance interactions leading to a necessity to use much more effective parameters. The lack of experimental information on the highly vibrationally excited interacting states of the HDO molecule also presents a serious obstacle in implementation of the EH approach.

The above-mentioned reasons prevented complete identification and modeling of the high resolution spectrum of HDO. For example, many weak lines were left unassigned in the Fourier transform spectrum recorded and analyzed in the 7600–8100 cm^{-1} spectral region in [5]. Meanwhile, the prediction power of the SP calculation has proved to be highly helpful in the line-by-line analysis for HDO spectra in many regions [6–11]. In this paper, we present a new theoretical and experimental study of the Fourier transform absorption spectrum of HDO in the region 7500–8200 cm^{-1}. This time in the identification process we rely mainly on the SP calculation, which seems to be also very accurate in the considered spectral region.

As will be seen from the forthcoming sections, application of the detailed and accurate theoretical linelist to more extensive and accurate experimental data

☆ Supplementary data for this article are available on ScienceDirect (www.sciencedirect.com) and as part of the Ohio State University Molecular Spectroscopy Archives (http://msa.lib.ohio-state.edu/jmsa_hp.htm).

* Corresponding author. Fax: +86-551-360-2969.
E-mail address: smhu@ustc.edu.cn (S.-M. Hu).

0022-2852/$ - see front matter © 2004 Elsevier Inc. All rights reserved.
doi:10.1016/j.jms.2004.06.002

recorded at a higher resolution and better signal-to-noise ratio resulted in retrieval of large set of new experimental energy levels for the (3 0 0), (0 3 1), and (1 1 1) vibrational states of HDO compared to [5].

2. Experimental details

The sample of $D_2{}^{16}O$ was purchased from PeKing Chemical Industry, (China). The stated purity of deuterium was 99.8%. The HDO sample was prepared by mixing the D_2O and H_2O in the a ratio of 1:1. The spectra were recorded at room temperature (296 K) with the Bruker IFS 120HR Fourier-transform interferometer (Hefei, China), which was equipped with a path length adjustable multi-pass gas cell, a tungsten source, a CaF_2 beam-splitter, and Ge diode detector. The unapodized resolution was $0.01\,cm^{-1}$ and the apodization function was Boxcar. The sample pressure was 10 hPa which was measured by a manometer with a stated accuracy of 20 Pa. The total path length was 87 m. To improve the signal-to-noise ratio, 2040 scans were accumulated.

Since in the region under study there are many absorption lines due to the H_2O and D_2O, the spectrum of "pure" D_2O was also recorded to identify the absorption lines of HDO. The spectrum was calibrated with H_2O lines in this region listed in the Hitran database. The precision in the positions of unblended lines was estimated better than $1 \times 10^{-3}\,cm^{-1}$. For illustration, a small piece of the recorded spectra is presented Fig. 1.

3. Spectrum assignment and energy level derivation

For identification purpose, approximate intensities were derived for each observed line from the peak absorption values. Synthetic HDO spectrum from [1,2] was used as the input data for the expert system for automatic assignment of the rovibrational molecular spectra.

Since a large number of observed energy levels were derived from a single line without ground state combination differences (GSCD), it is worth to gives some details of the identification process here. Obviously, the reliable identification of single lines entirely depends on the accuracy of the simulated spectrum used in the assignment process. To the best of our knowledge, the SP prediction of the line positions and intensities of water vapor and its isotope species is one of the most accurate among recent ab initio and variational calculations, at least for wavenumbers lower than $16\,000\,cm^{-1}$. Although the accuracy of the SP calculation of line positions varies significantly depending on the spectral region, isotope species, and vibrational band considered (see, for example, [12]), these variations behave regularly with the V_1, V_2, V_3 vibrational, and the J, K_a rotational quantum numbers. This gives the opportunity to introduce the correcting factor for SP prediction for each vibrational band.

Another important point in the weak line identification process is the matching between the observed and calculated intensities. In case of intensity consideration, one should estimate an intensity threshold—I_1 in calculated data which means that all calculated lines with

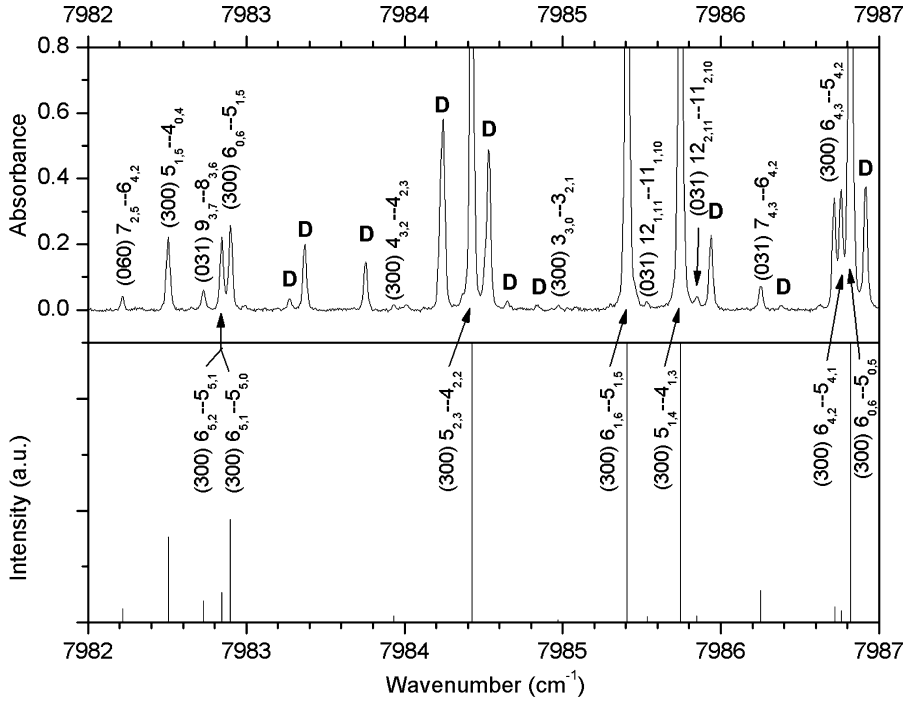

Fig. 1. Part of the spectrum of HDO. Upper panel: observed spectrum; Lower panel: stick spectrum from ab initio calculation by Schwenke and Partridge [1,2]. Transitions of HDO are assigned while D_2O lines are indicated with "D." Note that some strong lines are beyond the display range.

$I \geqslant I_1$ should be observed in the spectrum or their absence can be explained by the overlapping with stronger lines in their vicinity. Another threshold—I_2 can be introduced for the weakest lines, so all calculated lines with intensity $I_2 \leqslant I < I_1$ either can be found or be absent in the spectrum, and all calculated lines with intensity $I < I_2$ can be neglected. Obviously, that I_2 should be close to the noise level of the spectrum. On the other hand, we should not find in the observed spectrum those lines, which cannot be explained within the estimated accuracy of the synthetic spectrum. If these rules hold for simulated spectrum, one can rely on this calculation without running the risk of making a wrong assignment.

The synthetic spectrum for considered spectral region was found to be of a high quality. In Table 1 an average and maximum deviation between the observed and calculated positions is presented for all considered vibrational states of HDO in this region. As shown in Table 1, the averaged deviations for most of the analyzed states do not exceed 0.07 cm^{-1}, that is quite satisfactory for the unambiguous line identification since we found that the observed and calculated values of line intensities also match well. In our case, the I_2 and I_1 values were estimated to be of 5.0E−07 and 4.0E−06 $cm^{-2}\,atm^{-1}$, respectively. Comparison of the observed and calculated spectrum in the whole region is shown in Fig. 2.

Finally 1254 absorption lines of HDO were rotationally assigned and they correspond to 1415 transitions going on five upper vibrational states (see Table 1). The resulting linelist, which includes observed HDO line positions and calculated [2] intensities followed by rovibrational assignment, is attached to this paper as Supplementary material. The HDO lines blended by the D_2O lines are specially marked. Some relatively strong HDO lines were not included into the linelist since they are unrecoverably blended by stronger lines of other isotope species.

Extensive set of 508 precise experimental energy levels of HDO was derived by adding the ground state experimental energy levels [13] to the observed transitions.

Table 1
Deviations between the observed and calculated (SP [1,2]) energy levels for the HDO vibrational states in the considered region

V_1	V_2	V_3	Band center (cm^{-1})		No. of observed levels		$E_{obs} - E_{calc}$ (cm^{-1})	
			E_{obs}	E_{calc}	This work	Ref. [5]	Average	Maximum
0	0	2	7250.5192	7250.640	102		0.14	−0.22
0	3	1	7754.6055	7754.630	111	11	0.00	±0.03
1	1	1	7808.7586	7808.730	103	37	0.01	+0.04
0	6	0	7914.3170	7914.365	10	2	0.03	−0.06
3	0	0	7918.1719	7918.135	164	83	0.06	−0.18
2	2	0		8090.034	18		0.07	+0.10

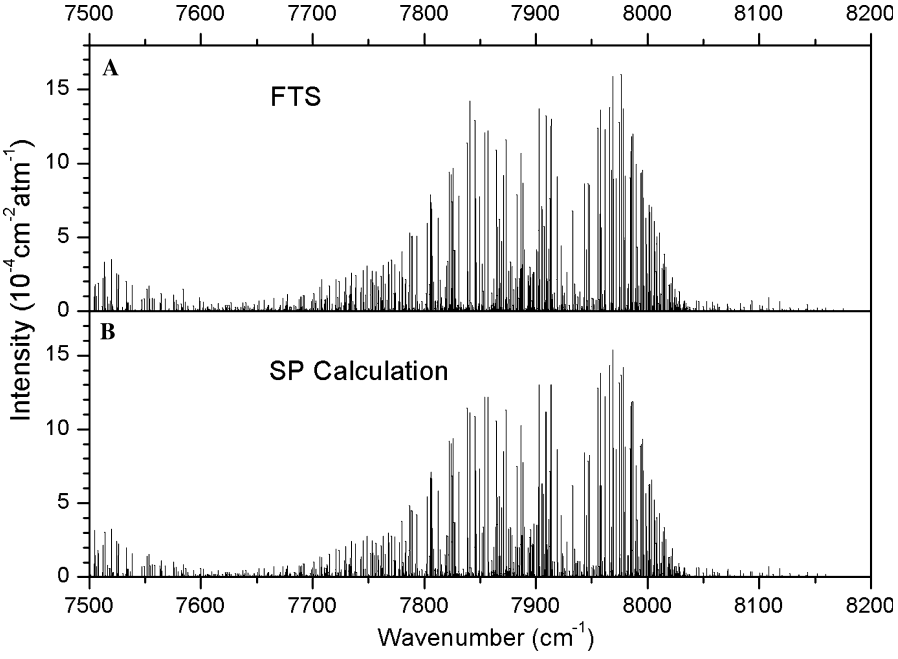

Fig. 2. Overview of the HDO spectrum between 7500 and 8200 cm^{-1}. (A) Stick spectrum retrieved from the FTS spectrum recorded with a 87 m absorption path length at a total pressure of water of 10 hPa (D:H ≈ 1:1). (B) Stick spectrum from ab initio calculation by Schwenke and Partridge [1,2].

Table 2
Rotational energy levels (in cm^{-1}) of the (3 0 0), (0 3 1), and (1 1 1) vibrational states of HDO

J	K_a	K_c	E_{obs} cm^{-1} (3 0 0)	$\sigma \times 10^3$ cm^{-1}	N	E_{obs} cm^{-1} (0 3 1)	$\sigma \times 10^3$ cm^{-1}	N	E_{obs} cm^{-1} (1 1 1)	$\sigma \times 10^3$ cm^{-1}	N
0	0	0	7918.1719		1	7754.6055		1	7808.7586		1
1	0	1	7932.8872	0.1	2	7770.0448	0.6	2	7824.1053	2.6	2
1	1	1	7946.6145	0.7	2	7789.2029	0.2	2	7840.9318	0.1	2
1	1	0	7949.0716	0.1	2	7792.4604	0.3	2	7843.9931	0.4	2
2	0	2	7962.2634	0.3	3	7800.5240	0.2	3	7854.4164	0.2	2
2	1	2	7973.4633	0.6	3	7816.7599	0.1	3	7868.5855	0.2	3
2	1	1	7980.8263	0.3	4	7826.5117	0.6	2	7877.7446	0.1	2
2	2	1	8022.6185	0.2	2	7929.4767	0.1	2	7880.7671	0.1	4
2	2	0	8022.9129	0.2	4	7929.8454	0.1	2	7881.1278	0.5	3
3	0	3	8004.2474	0.1	3	7845.2879	1.2	3	7898.9523	0.8	2
3	1	3	8013.5499	0.1	4	7857.8590	0.1	2	7909.8405	0.1	3
3	1	2	8028.2391	0.1	4	7877.2686	1.1	2	7928.3441	0.2	3
3	2	2	8066.5185	0.1	5	7975.7249	0.1	3	7926.5378	0.2	4
3	2	1	8067.9604	0.4	5	7977.5292	0.4	2	7928.5832	0.4	6
3	3	1	8142.0179	0.1	2	8073.9264	2.5	2	8017.0379	0.1	3
3	3	0	8142.0393	0.2	2	8074.0623	1.1	3	8017.0678	0.3	2
4	0	4	8060.2222	0.2	3	7903.3697	0.3	3	7956.8161	0.2	3
4	1	4	8066.6864	0.3	3	7912.2573	0.1	2	7964.4609	0.3	2
4	1	3	8091.0188	0.1	3	7944.3139	0.1	2	7994.9607	0.1	2
4	2	3	8124.7992	0.2	4	8037.0823	0.1	3	7987.5453	0.4	3
4	2	2	8128.9428	0.3	9	8042.2400	0.1	2	7993.0072	0.2	2
4	3	2	8200.9727	0.1	4	8136.5558	0.4	2	8078.5373	0.3	3
4	3	1	8201.1254	0.1	3	8136.4740	0.1	2	8078.7557	0.3	3
4	4	1	8305.1165	0.2	2	8275.8404	0.2	3	8194.5927	0.4	3
4	4	0	8305.1156	0.7	2	8275.8384	0.3	2	8194.5919	0.6	2
5	0	5	8128.5183	0.1	3	7973.9086	0.9	3	8027.2378	0.1	2
5	1	5	8132.6631	0.2	3	7979.6895	0.3	2	8032.1865	0.1	2
5	1	4	8168.7285	0.1	3	8027.0248	0.1	2	8077.4149	0.2	2
5	2	4	8197.2465	0.2	3	8113.2939	0.3	2	8063.1567	0.4	4
5	2	3	8206.2607	0.1	6	8124.3820	0.1	3	8074.8498	0.6	4
5	3	3	8274.7739	0.2	6	8214.9765	0.4	2	8155.5026	1.6	2
5	3	2	8275.3689	0.4	5	8215.4116	0.2	2	8156.3555	0.6	2
5	4	2	8378.6132	0.4	3	8354.2027	1.0	3	8271.0682	1.1	2
5	4	1	8378.6254	0.1	3	8354.2614	0.2	2	8271.0753	0.7	3
5	5	1	8510.9579	0.4	2	8530.6453	0.2	2	8413.6540	0.6	2
5	5	0	8510.9563	0.2	2	8530.6468	1.2	2	8413.6530	0.3	2
6	0	6	8208.7655	0.2	4	8056.3869	0.1	2	8109.7735	0.3	3
6	1	6	8211.2727	0.1	4	8059.8977	0.1	2	8112.7750	0.1	2
6	1	5	8260.7653	0.3	3	8124.5504	0.6	3	8174.9171	0.1	2
6	2	5	8283.6025	0.2	3	8204.0516	0.4	3	8153.0928	0.1	2
6	2	4	8299.9813	0.2	4	8222.9915		1	8174.1073	1.6	4
6	3	4	8363.6432	0.1	3	8309.1418	0.2	3	8247.7629	0.6	3
6	3	3	8365.1502	0.1	4	8310.8843	0.2	2	8250.3224	1.0	4
6	4	3	8466.9589	0.2	4	8448.3924	0.3	3	8362.9616	0.1	2
6	4	2	8467.0205	0.4	2	8448.7355	0.2	2	8362.8178	0.2	2
6	5	2	8598.8148	0.1	2	8624.4269	1.1	2	8505.0336	0.2	2
6	5	1	8598.8142	0.7	2	8624.4263	1.7	2	8505.0341	0.7	2
6	6	1	8759.0094	0.1	3	8833.1236		1	8674.2375		1
6	6	0	8759.0094	0.1	3	8833.1236		1	8674.2375		1
7	0	7	8300.9173	0.1	5	8150.6417	0.2	2	8204.2820	0.2	2
7	1	7	8302.3484	0.3	3	8152.6679	0.5	2	8206.0152	0.1	2
7	1	6	8366.3833	0.4	5	8286.5722	1.3	2	8235.8491		1
7	2	6	8383.5814	0.1	4	8309.0149	0.1	2	8256.9764	0.2	2
7	2	5	8409.8214	0.1	4	8342.9073		1	8290.3012	2.5	2
7	3	5	8466.5714	0.1	2	8418.9312		1	8355.8086	0.1	4
7	3	4	8471.1290	0.4	5	8423.4728	0.6	2	8361.2035	0.5	2
7	4	4	8570.2377	0.1	3	8558.3956	0.1	2	8470.1379	0.2	2
7	4	3	8570.4518	0.2	4	8560.2253	2.4	3	8470.8922	0.2	3
7	5	3	8701.4024	0.8	2				8611.7671		1
7	5	2	8701.4052	0.7	2	8733.9465		1	8611.7782	0.5	2
7	6	2	8861.0423	0.2	2	8942.2256	3.0	2	8780.3866	0.3	2
7	6	1	8861.0426	0.1	2	8942.2256	3.0	2	8780.3860	0.2	2

Table 2 (*continued*)

J	K_a	K_c	E_{obs} cm^{-1} (3 0 0)	$\sigma \times 10^3$ cm^{-1}	N	E_{obs} cm^{-1} (0 3 1)	$\sigma \times 10^3$ cm^{-1}	N	E_{obs} cm^{-1} (1 1 1)	$\sigma \times 10^3$ cm^{-1}	N
7	7	1	9047.9232	0.2	2				8975.4544	1.2	2
7	7	0	9047.9232	0.2	2				8975.4544	1.2	2
8	0	8	8404.9487	0.1	2	8256.7045	0.2	2	8310.7838	0.2	2
8	1	8	8405.7394	0.1	2	8257.8295		1	8311.7476	1.0	2
8	1	7	8484.6326	0.2	2	8411.4595	0.8	2	8359.8175	0.2	3
8	2	7	8496.8835	0.2	3	8427.8272	0.6	2	8374.4107	0.3	3
8	2	6	8535.2616	0.2	3	8476.6489		1	8422.4980	0.1	2
8	3	6	8584.4192	0.2	3	8544.1189	0.6	2	8479.1498	1.6	2
8	3	5	8592.5515	0.3	4	8553.7271	0.1	2	8489.6431	1.4	2
8	4	5	8688.7211	0.2	3	8683.9150	0.1	2	8593.8321	0.1	3
8	4	4	8689.2931	0.2	3	8683.9889	0.1	2	8594.5139	0.2	2
8	5	4	8818.7628	0.6	3	8859.1147		1	8733.9143		1
8	5	3	8818.7818	0.4	2	8859.1941		1	8733.9481		1
8	6	3	8977.7104	1.8	2	9066.9427		1	8901.7761	2.7	3
8	6	2	8977.7069	1.6	2	9066.9427		1	8901.7787	0.6	2
8	7	2	9163.9544		1				9096.2111		1
8	7	1	9163.9544		1				9096.2111		1
8	8	1	9376.6430		1						
8	8	0	9376.6430		1						
9	0	9	8520.9219	0.9	2	8374.6501		1	8429.3253	0.2	3
9	1	9	8521.3455	0.1	2	8375.2576	0.5	2	8429.8443	0.1	3
9	1	8	8615.0643	0.3	2	8548.8015	0.5	2	8495.5755		1
9	2	8	8623.1552	0.4	2	8560.1306	2.1	2	8505.0147	1.9	2
9	2	7	8675.6248	0.1	3	8627.7840	1.3	2	8571.4422	1.8	2
9	3	7	8716.5584	0.2	2	8684.3500	0.1	2	8615.4950		1
9	3	6	8731.2516	0.4	2	8701.9607	8.4	2	8635.6543	2.1	2
9	4	6	8820.5873	0.8	2				8732.4949	1.0	2
9	4	5	8822.0998	0.1	3				8734.4312		1
9	5	5	8950.9577	1.0	2	9000.0916		1	8871.5066		1
9	5	4	8951.0087		1				8871.6331		1
9	6	4	9109.0289	3.1	2	9207.2868		1			
9	6	3	9109.0343	1.8	2	9207.2873		1			
9	7	3	9294.5122	0.3	2						
9	7	2	9294.5119	0.5	2						
9	8	2	9506.4541		1						
9	8	1	9506.4541		1						
9	9	1	9744.0518		1						
9	9	0	9744.0518		1						
10	0	10	8648.8589	0.1	2	8504.5555		1	8559.9499	0.1	2
10	1	10	8649.0817	0.3	4	8504.8664		1	8560.2212	0.1	2
10	1	9	8757.1060	0.7	3	8698.1163	1.4	2	8642.7237		1
10	2	9	8762.1923	1.3	2	8705.6028	0.1	2			
10	2	8	8830.0581	0.9	2	8793.0070	0.6	2			
10	3	8	8862.6989	0.1	2	8839.8877		1	8767.1630		1
10	3	7	8887.4378	0.3	2	8867.9057	3.0	2	8799.0637		1
10	4	7	8968.7028	1.0	2				8885.7178		1
10	4	6	8972.1544	0.3	2	8987.4482		1	8891.0983	1.1	2
10	5	6	9097.9584	0.5	2						
10	5	5	9098.1687	0.5	2	9157.3095		1	9024.9251		1
10	6	5	9255.0239		1	9363.2540		1			
10	6	4	9255.0346		1	9363.2567		1			
10	7	4	9439.6070		1						
10	7	3	9439.6071		1						
11	0	11	8788.7708	0.1	2	8646.4372		1			
11	1	11	8788.8868	0.3	2	8646.6004		1	8702.8109	0.2	2
11	1	10	8910.6516	0.2	2	8859.1970		1			
11	2	10	8913.7058	0.4	2	8863.9556	1.8	2			
11	2	9	8997.8507	0.8	2	8973.9347		1			
11	3	9	9022.5648	0.1	2	9008.8965		1			
11	3	8	9059.1873	0.6	2	9049.9359		1			
11	4	8	9131.2681	0.2	2	9158.3159		1			
11	4	7	9138.1446	0.4	2						
11	5	7	9259.8456	0.8	2						

Table 2 (*continued*)

J	K_a	K_c	E_{obs} cm^{-1} (3 0 0)	$\sigma \times 10^3$ cm^{-1}	N	E_{obs} cm^{-1} (0 3 1)	$\sigma \times 10^3$ cm^{-1}	N	E_{obs} cm^{-1} (1 1 1)	$\sigma \times 10^3$ cm^{-1}	N
11	5	6	9260.3898		1						
11	6	6	9415.7669		1						
11	6	5	9415.7772		1						
11	7	5	9599.2361		1						
11	7	4	9599.2363		1						
12	0	12	8940.6520	0.4	2				8857.4994	0.1	2
12	1	12	8940.7067	1.6	2				8857.5771		1
12	1	11	9075.7355	0.3	3	9032.0095		1			
12	2	11	9077.4934		1	9034.9726		1			
12	2	10	9178.0456		1	9164.7969		1			
12	3	10	9196.3503		1	9191.3435		1			
12	3	9	9244.5555		1						
12	4	9	9308.2763		1						
12	4	8	9320.6861		1						
12	5	8	9436.6126		1						
12	5	7	9437.8584		1						
12	7	6	9773.4386		1						
12	7	5	9773.4396		1						
13	0	13	9104.4639		1				9024.3994		1
13	1	13	9104.5117		1				9024.4472		1
13	1	12	9252.4347	4.3	2	9216.6782		1			
13	2	12	9253.4422		1	9218.5109		1			
13	2	11	9367.1298		1						
13	3	11	9380.7672		1						
13	3	10	9447.6649		1						
13	4	10	9499.4768		1						
13	4	9	9519.9991		1						
13	5	9	9628.1676		1						
14	0	14	9280.2049		1						
14	1	14	9280.2253	3.6	2						
14	1	13	9440.8411	0.8	2						
14	2	13	9441.3939		1						
14	2	12	9571.6776		1						
14	3	11	9663.2365		1						
15	0	15	9467.8220	1.1	2						
15	1	15	9467.8293	3.2	2						
15	2	14	9641.3298		1						
16	0	16	9667.2765		1						
16	1	16	9667.2817		1						

N is the number of lines used for the upper energy level determination and σ denotes the corresponding experimental uncertainty in 10^{-3} cm^{-1}.

This number should be compared with 135 energy levels obtained in [5] (see Table 1). The observed energy level values are presented in Tables 2 and 3 together with the experimental uncertainties and number of lines used for level determination. As a comparison, the experimental uncertainty indicated by the GSCD method is about 4×10^{-4} cm^{-1} on average, which is significantly better than in our previous contribution [5]. For the (0 0 2) state earlier investigated in [14], only 22 new (compared to [14]) energy levels are shown of 102 observed.

As it was stressed in [5], the strong interaction between the (0 3 1) and (1 1 1) vibrational states results in greatly mixed wave-functions and ambiguity in vibrational assignment of their rotational levels. We accepted here the rovibrational assignments proposed by SP, which may differ in some cases from those given in [5]. An interesting example of the high-order local rovibrational resonance represents the (3 0 0)–(0 6 0) interaction. This coupling affects the $K_a = 0$ energy levels of both states and induces reasonable intensity transfer to the otherwise extremely weak transitions of the $6\nu_2$ band. As J and K_a increase, the (0 3 1)–(0 6 0) coupling also becomes important. In addition to [5] data, we could derive eight energy levels of the highly excited (0 6 0) state (see Table 3) with $K_a = 0$, 1, and 2 including the band center at 7914.3170 cm^{-1}.

At the final stage of the spectrum analysis, we could partly assign transitions of the very weak (2 2 0)–(0 0 0) band. Eighteen energy levels were derived for the (2 2 0) vibrational state, which seemed to be strongly perturbed by resonance coupling with other states. In particular, the high K_a energy levels of the (3 0 0) state (not observed in [5]) are strongly coupled to the corresponding levels of the (2 2 0). The (0 0 2) energy levels have the largest average and maximum deviations from the SP prediction (see Table 1). However, these deviations vary

Table 3
Rotational energy levels (in cm^{-1}) of the (0 6 0), (0 0 2), and (2 2 0) vibrational states of HDO

J	K_a	K_c	E_{obs} (cm^{-1})	$\sigma \times 10^3$ cm^{-1}	N
			(0 6 0)		
0	0	0	7914.3170		1
1	0	1	7929.8972		1
2	0	2	7960.5925	0.3	3
3	0	3	8007.4630	0.3	3
4	0	4	8067.8172	0.8	2
4	1	3	8141.4562		1
5	0	5	8142.0631		1
6	0	6	8230.5251	2.0	3
7	1	7	8347.0643		1
7	2	5	8556.1889	0.6	3
			(2 2 0)		
2	2	0	8225.1342		1
3	0	3	8178.9222		1
3	2	2	8270.0021		1
4	0	4	8236.0140		1
4	2	2	8335.0522		1
4	4	1	8558.7081		1
4	4	0	8558.7062		
5	0	5	8305.5911		
5	2	4	8404.7408		
5	2	3	8415.1744		
5	5	1	8800.9838		
5	5	0	8800.9838		
6	1	6	8392.7248		
6	1	5	8455.8198		
7	0	7	8480.4521		
7	1	7	8484.1664		
8	0	8	8585.4354		1
9	0	9	8702.1795		1
			(0 0 2)	15	3
10	8	3	8926.9617		1
10	8	2	8926.9644		1
11	8	4	9094.5143		1
11	8	3	9094.5141		1
12	5	7	8794.9786	0.3	2
12	8	5	9277.2901		1
12	8	4	9277.2891		1
12	9	4	9485.5166		1
12	9	3	9485.5166		1
13	2	11	8750.3185		1
13	7	6	9290.6896		1
13	8	6	9475.2787		1
13	8	5	9475.2755		1
13	9	5	9682.4269		1
13	9	4	9682.4269		1
14	4	10	9139.4178		1
14	5	9	9223.0272	0.5	2
15	3	12	9298.8667		1
15	4	11	9383.7530		1
15	5	11	9441.3283		1
15	5	10	9463.5777		1
15	6	10	9577.6308		1

N is the number of lines used for the upper energy level determination and σ denotes the corresponding experimental uncertainty in 10^{-3} cm^{-1}. For the (0 0 2) state only 22 new (compared to [14]) energy levels are shown of 102 observed.

very slowly and regularly with J and K_a that allowed us to perform reliable assignments which were also confirmed by the EH calculations [15].

4. Conclusion

Usage of the high accuracy Schwenke and Partridge [1,2] calculation for the theoretical treatment of the Fourier transform absorption spectrum of HDO molecule in the 7500–8200 cm^{-1} spectral region provided complete assignment of the experimental data and derivation of the extensive set of new precise energy levels for the (3 0 0), (0 3 1), and (1 1 1) states. Some additional energy levels were also obtained for the highly excited (0 6 0) and (2 2 0) states. This new HDO energy level set represents enlargement of the existing data and can be used in further refinement of the water vapor potential function, while detailed HDO absorption linelist in the 7500–8200 cm^{-1} spectral region supplements the information contained in the spectroscopic databases like HITRAN compilation.

Acknowledgments

This work is jointly supported by the National Natural Science foundation of China (20103007, 50121202), and INTAS foundation (Project 03-51-3394). O.N. acknowledges the financial support from the Russian Foundation for Basic Researches (Grants Nos. 02-03-32512 and 02-07-90139).

References

[1] H. Partridge, D.W. Schwenke, J. Chem. Phys. 106 (1997) 4618–4639.
[2] D.W. Schwenke, H. Partridge, J. Chem. Phys. 113 (2000) 6592–6597.
[3] O.L. Polyansky, A.G. Császár, S.V. Shirin, N.F. Zobov, P. Barletta, J. Tennyson, D.W. Schwenke, P.J. Knowles, Science 299 (2003) 539–542.
[4] S.V. Shirin, O.L. Polyansky, N.F. Zobov, P. Barletta, J. Tennyson, J. Chem. Phys. 113 (2000) 6592–6597.
[5] S.-M. Hu, O.N. Ulenikov, G.A. Onopenko, E.S. Bekhtereva, S.-G. He, X.-H. Wang, H. Lin, Q.-S. Zhu, J. Mol. Spectrosc. 203 (2000) 228–234.
[6] O. Naumenko, A. Campargue, J. Mol. Spectrosc. 199 (2000) 59–72.
[7] O. Naumenko, E. Bertseva, A. Campargue, D. Schwenke, J. Mol. Spectrosc. 201 (2000) 297–309.
[8] E. Bertseva, O. Naumenko, A. Campargue, J. Mol. Spectrosc. 203 (2000) 28–36.
[9] A. Campargue, E. Bertseva, O. Naumenko, J. Mol. Spectrosc. 204 (2000) 94–105.
[10] E. Bertseva, O. Naumenko, A. Campargue, J. Mol. Spectrosc. 221 (2003) 38–46.
[11] O. Naumenko, S.-M. Hu, S.-G. He, A. Campargue, Phys. Chem. Chem. Phys. 6 (2004) 910–918.
[12] B. Voronin, Russian Phys. J. 43 (1999) 96–100.
[13] R. Toth, J. Mol. Spectrosc. 162 (1993) 20–40.
[14] R. Toth, J. Mol. Spectrosc. 186 (1997) 66–89.
[15] A. Bykov, O. Naumenko, T. Petrova, A. Scherbakov, L. Sinitsa, Atmos. Oceanic Opt. 11 (1998) 1281–1289.